Critical point dewetting observed in the liquid Se–Tl system on a quartz substrate

2006 J. Phys.: Condens. Matter 18 8449

(http://iopscience.iop.org/0953-8984/18/37/005)

INSTITUTE OF PHYSICS PUBLISHING JOURNAL OF PHYSICS: CONDENSED MATTER

J. Phys.: Condens. Matter **18** (2006) 8449–8469 doi:10.1088/0953-8984/18/37/005

Critical point dewetting observed in the liquid Se–Tl system on a quartz substrate

Y Ohmasa, S Takahashi, K Fujii, Y Nishikawa and M Yao

Department of Physics, Graduate School of Science, Kyoto University, Kyoto 606-8502, Japan

E-mail: ohmasa@scphys.kyoto-u.ac.jp

Received 19 July 2005
Published 29 August 2006
Online at stacks.iop.org/JPhysCM/18/8449

Abstract

We have studied the wetting phenomena of the liquid Se–Tl system on a quartz substrate by photography and ellipsometry, and found that a thin layer of the Se-rich liquid phase intrudes between the Tl-rich liquid phase and the quartz substrate in the temperature region far below the critical temperature. Surprisingly, neither the Se-rich nor the Tl-rich wetting film is formed near the critical temperature, indicating the critical point dewetting. In addition, we found that the temperature difference between the surface and the bulk liquid induces the transition between the wetting and non-wetting states. In order to interpret the observation, we constructed a model grand potential, incorporating the long-range interaction, the temperature difference and gravity. From this analysis, it is suggested that the combination of the long-range force and gravity plays an important role in overcoming the critical point wetting phenomena.

(Some figures in this article are in colour only in the electronic version)

1. Introduction

In 1977, Cahn predicted critical point wetting on the basis of short-range interatomic interactions and the mean field theory [1]. He argued that complete wetting takes place inevitably in any three-phase system when the temperature is sufficiently close to the critical point, where two of the three phases become indistinguishable. For example, when the three-phase system consists of vapour, liquid droplet and solid substrate, the critical point under consideration is the liquid–vapour critical point. Another important three-phase system is an immiscible binary liquid system (say, A–B mixture) on a substrate, and its relevant critical point is the upper consolute point of the binary liquids, where the two liquids become miscible. In this case, a wetting film of one of the two coexisting liquid phases (for example, the A-rich phase) intrudes between the other liquid phase (B-rich phase) and the substrate when the critical point is approached.

Cahn's theoretical predictions have been confirmed for many fluid systems experimentally [3]. For example, wetting transitions in binary systems against a solid wall [4, 5] were observed. Furthermore, other possibilities, such as 'critical point drying', 'critical point partial drying' and 'absence of critical point wetting', have been predicted theoretically.

In 1982, Nakanishi and Fisher [2] examined wetting transitions in detail using a Cahn–Landau squared-gradient theory based on the short-range interaction, and produced a global phase diagram in the space of temperature, chemical potential, short-range surface field h_1 and surface coupling enhancement. It is noticed that their phase diagram is symmetric with respect to $h_1 = 0$, and 'critical point drying' appears in the $h_1 < 0$ region as a counterpart of the critical point wetting in the $h_1 > 0$ region. In the case of the A–B liquid binary system on a substrate, 'wetting' means that the substrate is covered by one of the two liquid phases (A-rich phase), while 'drying' means that it is covered by the other liquid phase (B-rich phase).

In 1987, Ebner and Saam indicated that critical point wetting or drying does not necessarily occur when the long-range interaction is taken into account [6]. For example, if the short-range force prefers drying and the long-range force prefers wetting, a transition between two states of incomplete drying (i.e. a 'partial drying' transition) will take place for a strong enough short-range surface field h_1. If h_1 is weak, on the other hand, they predicted that neither critical point wetting nor drying occurs up to the critical temperature T_c. This prediction was confirmed experimentally by Durian and Franck [7] and Abeysuriya *et al* [8], who studied binary liquid mixtures at coexistence on a silylated borosilicate glass substrate.

In addition to these unusual wetting phenomena, the possibility of 'critical point dewetting' has been pointed out [9–11]. This is accompanied by a phase transition from complete to partial wetting as the critical point is approached. In the case of the A–B liquid binary system, an A-rich (or B-rich) wetting film is formed when the temperature is far below the critical temperature, and, when the critical point is approached, it disappears. This 'critical point dewetting' is a completely opposite phenomenon to Cahn's critical point wetting (i.e. formation of an A-rich wetting film near the critical point), and is also different from 'drying' (i.e. formation of a B-rich wetting film near the critical point). From the purely theoretical point of view, Indekeu indicated that 'critical point dewetting' is possible even in a system with only short-range forces, when the surface field is specially chosen [9]. Experimentally, however, 'critical point dewetting' remains controversial. Early measurements showed a sudden decrease in the thickness of the wetting film below the critical point in the liquid–vapour interface of the cyclohexane–methanol–water system [10] and the liquid–glass interface of the nitromethane–carbon disulfide system [11], and these measurements may be related to the critical point dewetting. Recent papers [12, 13] are, however, opposed to these results. They pointed out that it is not clear whether true equilibrium was reached in these studies, because the metastable states have long lifetime, and therefore the results are not conclusive.

In the present work, we have studied the wetting phenomena of the liquid Se–Tl system on a quartz substrate by photography and ellipsometry. The liquid Se–Tl system has a miscibility gap in the Se-rich region with a critical point at $T_c = 454\,^{\circ}\mathrm{C}$ and $X_c = 92.05$ at.% Se [14, 15]. We observed that a thin layer of the Se-rich liquid phase intrudes between the Tl-rich liquid phase and the quartz substrate. Surprisingly, neither a Se-rich nor a Tl-rich wetting film is formed near the critical temperature, but is formed in the lower temperature region. Namely, 'critical point dewetting' is observed.

Liquid Se–Tl is a particularly interesting system, because it is a mixture of a semiconductor (liquid Se) and a metal (liquid Tl), and the phase-separated Se-rich and Tl-rich phases have substantially different electronic and dielectric properties [14]. In this situation, dramatic changes in wetting behaviour are expected because long-range interactions between the wetting

film and the substrate depend strongly on the dielectric permittivity. Another example of the interplay between the dielectric property and the wetting transition is observed in the system of fluid mercury on sapphire substrate. This system shows both the metal–non-metal transition and the wetting transition near the liquid–vapour critical point of mercury [16, 17]. Optical reflectivity measurements show that the density of the mercury wetting film is much smaller than that of the bulk liquid mercury, and the wetting film is in a non-metallic state [18].

Another important aspect of the liquid Se–Tl system is its large difference in the mass densities, $\delta\rho$, between the two coexisting liquid phases. For example, $\delta\rho \sim 1$ g cm^{-3} at $\sim$420 °C [15], and it is much larger than $\delta\rho$ in the nitromethane–carbon disulfide system ($\sim$0.1 g cm^{-3}) or in the cyclohexane–methanol system ($\sim 10^{-3}$ g cm^{-3}), which are usually used for critical point wetting experiments. Because of the large $\delta\rho$, the wetting film feels large gravitational potential, and this affects the wetting phenomena. Therefore, liquid Se–Tl is a unique system with a combination of large long-range force and large gravitational potential.

In addition to gravity, we introduced a temperature gradient as another external field to control the surface state of the system. As will be discussed in section 4.2, the temperature gradient can be used to shift the chemical potential near the surface from the two-liquid coexistence value, and this affects the wetting properties strongly. Therefore, it can be used to understand the equilibrium properties of the system, rather than to study the system out of equilibrium. In the present work, we found that the temperature difference between the surface and inside of the sample cell induces the transition between the wetting and the non-wetting states.

In order to interpret the unusual wetting phenomena observed in the liquid Se–Tl system, we have constructed a model grand potential incorporating the long-range force, the chemical potential induced by the temperature difference, and gravitational potential, and succeeded in reproducing the observed wetting behaviour qualitatively. From this analysis, we suggest that the combination of the long-range force and gravity plays the crucial role in overcoming the critical point wetting phenomena.

2. Experimental details

2.1. Sample preparation and the furnace

The experiment was carried out for the Se–Tl mixture with the critical component, $Se_{92.05}Tl_{7.95}$. Since thallium is very reactive to the air, the sample was treated under He atmosphere. Accurately weighted amounts of Tl (99.9% purity) and Se (99.99% purity) were melted and mixed at 500 °C in an evacuated quartz tube. After cooling, the sample was encapsulated in a quartz cell and then sealed off under vacuum. The quartz cell has a rectangular parallelepiped shape and one of the vertical flat surface was used as an optical window. Before filling the sample, the quartz cell was cleaned with a potassium dichromate solution, rinsed many times with pure water, and then dried. This sample preparation procedure plays a crucial role on the experimental results. For example, if the cleaning of the cell or removal of oxides on the thallium surface is not sufficient, a thin film of Tl-rich liquid phase is formed between the quartz substrate and the Se-rich liquid phase. On the other hand, if the sample is treated properly, a Se-rich film is formed between the Tl-rich phase and the quartz substrate. The discrepancy may be due to a contamination layer (perhaps oxides) on the quartz surface, which is suspected of attracting the Tl-rich phase.

The quartz cell was heated up in a furnace, and the interface between the liquid sample and the quartz wall was observed by a digital CCD camera (Minolta Dimage 7) and ellipsometric measurements. Figure 1 shows the heater assembly. It was designed to control the temperature

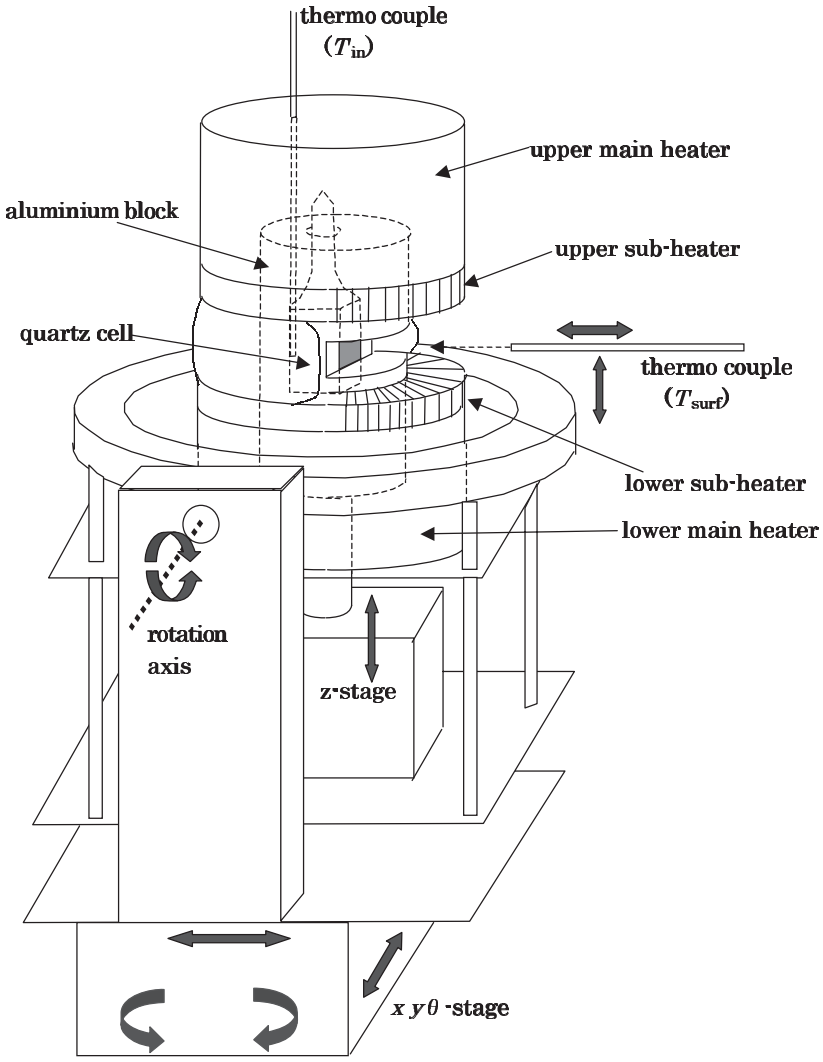

Figure 1. A schematic drawing of the heater assembly designed to control the temperature of the surface of the cell, T_{surf}, independently of that of the bulk liquid, T_{in}.

of the surface of the cell, T_{surf}, independently of that in the interior of the cell, T_{in}. The sample cell is embodied in an aluminium block whose temperature is controlled by two main heaters. T_{in} is measured by the thermocouple attached to the aluminium block side of the cell. The aluminium block has a slit, through which one can observe the surface of the cell. The temperature at the surface of cell, T_{surf}, is controlled by the two subsidiary (sub-) heaters. T_{surf} is measured by a thermocouple inserted through the slit and attached to the optical window of the cell. The position of the thermocouple can be changed by using an xyz-stage.

At the beginning of the experiment, the temperature of the sample was increased up to 550 °C, where the equilibrium state of the Se–Tl sample is in the single homogeneous liquid phase. In order to accelerate the equilibration process to the homogeneous state, the furnace was shaken several times using the rotation axis shown in figure 1. Then the temperature

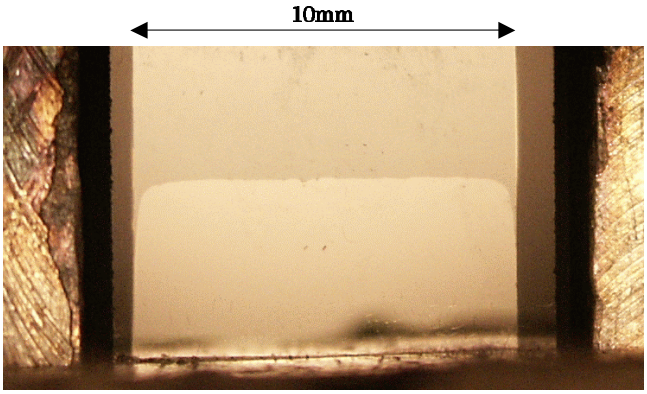

Figure 2. A photograph of the interface between the liquid sample and the quartz wall taken at $T_{surf} = 366\,^{\circ}C$ and $T_{in} = 352\,^{\circ}C$.

was decreased down into the two-phase region. Figure 2 shows an example of a photograph taken at $T_{surf} = 366\,^{\circ}C$ and $T_{in} = 352\,^{\circ}C$. The two phase-separated liquid phases can clearly be distinguished by the difference in the optical reflectivity (the Se-rich phase looks dark compared to the Tl-rich phase). The three-phase contact line is defined as the line that separates the interfaces between the two liquid phases and the quartz wall. The shape and position of the contact line characterizes the wetting property of the interface.

Because both liquid phases are optically opaque, only the liquid–quartz interface is observable. In this sense, this observation is surface-sensitive. As shown in the appendix, we have calculated the reflectivity of the Se-rich wetting film between the quartz substrate and the Tl-rich bulk phase as a function of the film thickness, and confirmed that a wetting film with a thickness of only a few tens of nanometres causes a large difference in the reflectivity because of the large difference in the complex refractive index between the wetting film and the bulk phase. Therefore, the existence of the wetting film can be easily detected by direct observation.

We observed the surface on changing the temperatures T_{in} and T_{surf}. In the present work, T_{in} and T_{surf} were changed only in the decreasing direction, because the time required for the bulk concentration to reach its equilibrium value is much shorter for the decreasing direction than the increasing direction. When the temperature jump is small enough ($\sim 2\,^{\circ}C$), the surface state reaches its steady state within 10–20 min. We then waited for about 1 h before taking the optical data. At a few state points near the critical temperature, we waited for 8–10 h, shaking the furnace several times, and confirmed that no further change was observed in the surface state. When the temperature jump is large (10–20 °C), on the other hand, some strange phenomena such as transient wetting are observed, and it took 1–2 h to reach the steady state. Details of the transient phenomena will be given elsewhere [19].

2.2. Ellipsometry

For the ellipsometric measurements, we adopted a rotating-analyser method [20]. We used a tungsten lamp as the light source. The light was focused onto the sample cell by using an aperture (1 mm in diameter) and a lens ($f = 200$ mm) through a polarizer. The size of the spot was ~ 2 mm at the sample position. The reflected light, passed through an analyser and optical fibres, was detected by multichannel spectrometers (Soma S-2600 and S-2700). They are equipped with a Si-CCD (wavelength range 350 nm $< \lambda <$ 1050 nm) and an

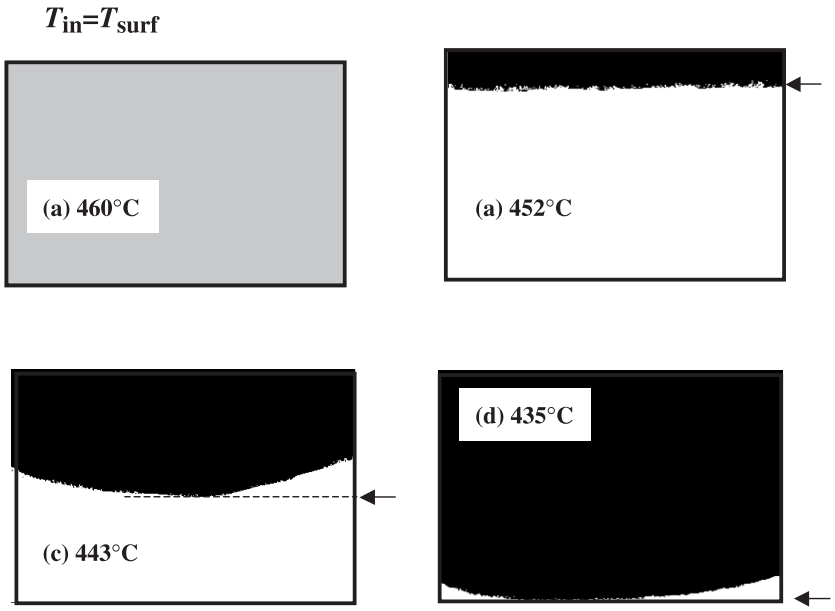

Figure 3. The binarized images of the liquid–quartz interface in the homogeneous temperature condition, $T_{surf} = T_{in} = 460\,°C$ (a), 452 °C (b), 443 °C (c) and 435 °C (d). The Se-rich, the Tl-rich and the supercritical one-phase regions are indicated by black, white and grey, respectively. Arrows indicate the height of the three-phase contact line.

InGaAs linear image sensor (900 nm $<\lambda<$ 1600 nm) as light detectors, respectively. The Stokes parameters $S_1(\lambda)$ and $S_2(\lambda)$ [21] were obtained as functions of the wavelength λ from the observed light intensity. $S_1(\lambda)$ and $S_2(\lambda)$ are related to the reflectivity ratio $\rho = r_p/r_s = \tan\psi \exp(i\delta)$ of p- and s-polarized light by $S_1 = -\cos 2\psi$ and $S_2 = \sin 2\psi \cos\delta$. The Stokes parameters were analysed using an oscillator-fit method to extract the complex dielectric function $\epsilon(\omega) = \epsilon'(\omega) + i\epsilon''(\omega)$ of the liquid sample. Details of the experimental setup and the analysis method will be given elsewhere [22].

3. Results

3.1. Wetting in the homogeneous temperature condition

Figure 3 shows photographs of the liquid–quartz interface in the homogeneous temperature condition, $T_{surf} = T_{in}$. For a visual aid, we have indicated binarized images. The surfaces covered with the Se-rich and Tl-rich phases are indicated by black and white, respectively. The supercritical one-phase region is indicated by grey. The sample temperature for figure 3(a) is 460 °C, which is higher than the critical temperature $T_c = 454\,°C$. In this condition, the liquid sample is in the single homogeneous phase (indicated by the grey region), and no contact line is observed. When the temperature is decreased below T_c, the liquid sample is separated into the Se-rich and the Tl-rich phases, and the contact line appears (figure 3(b)). When the temperature is decreased further, the contact line goes downward (figures 3(c) and (d)), and finally disappears again between 420 and 435 °C, indicating that the entire liquid–quartz interface is covered with the Se-rich phase. We have determined the height of the contact line as indicated by arrows in figure 3. The solid circles in figure 4 show the height h of the contact line relative to the bottom of the cell.

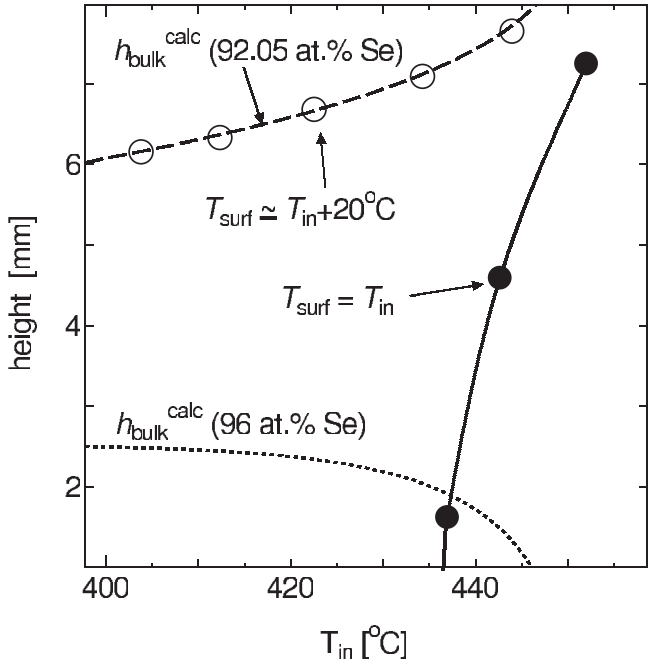

Figure 4. The observed height of the three-phase contact line relative to the bottom of the cell is denoted for $T_{surf} = T_{in}$ by the solid circles and for $T_{surf} \simeq T_{in} + 20\,^{\circ}\mathrm{C}$ by the open circles. The dashed and dotted lines are the position of the bulk meniscus h_{bulk}^{calc} for the critical composition sample (92.05 at.% Se) and for 96 at.% Se sample, respectively, calculated from the composition and the density data in [15]. The solid line is a guide for the eyes.

It should be emphasized that the observed temperature variation of the height of the contact line exhibits completely different behaviour from that of the bulk meniscus. This is true not only for the critical concentration but also for the off-critical concentration. Indeed, if the system has an off-critical concentration, the system should approach the single phase near the critical temperature. However, the present experiment shows completely opposite phenomena: two-phase separation is observed near the critical temperature, and only the Se-rich phase is visible apart from the critical temperature.

In figure 4, the positions of the bulk meniscus h_{bulk}^{calc} for the critical concentration sample (92.05 at.% Se) and that for the off-critical sample (96 at.% Se) are compared with the observed height of the contact line. They are calculated from the composition and the density data for the liquid Se–Tl system [15] as follows:

$$h_{bulk}^{calc} = \frac{c_{coex}^{Se-rich} - c_0}{c_{coex}^{Se-rich} - c_{coex}^{Tl-rich}} \frac{w_{Se} c_{coex}^{Tl-rich} + w_{Tl}(1 - c_{coex}^{Tl-rich})}{w_{Se} c_0 + w_{Tl}(1 - c_0)} \frac{W}{\rho_{coex}^{Tl-rich} S},$$

where $c_{coex}^{Se-rich}$ and $c_{coex}^{Tl-rich}$ are mole fractions of Se-component for the coexisting Se-rich and Tl-rich liquid phases, respectively, $w_{Se} = 78.96$ and $w_{Tl} = 204.37$ are the atomic weights, $\rho_{coex}^{Tl-rich}$ is the mass density of the Tl-rich liquid phase, W and c_0 are the weight and the Se mole-fraction of the initially prepared sample, respectively, and S is the horizontal cross-section of the quartz sample cell. As c_0 increases from the critical concentration, the h–T curve moves downward, and its slope and curvature change from positive to negative. None of these curves coincides with the present experimental result of h, which decreases rapidly with decreasing temperature.

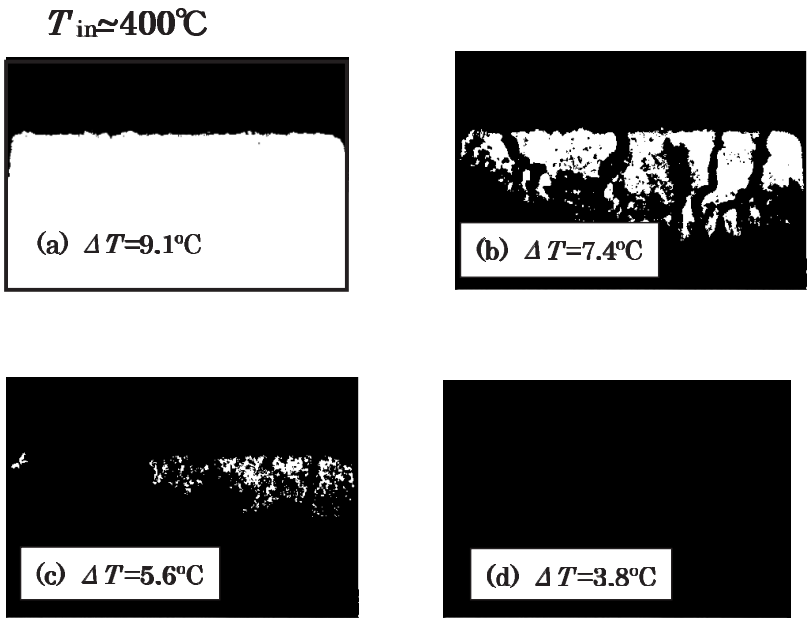

Figure 5. The binarized images of the liquid–quartz interface for various $\Delta T = T_{surf} - T_{in}$ at fixed T_{in} of 400 °C. The Se-rich and the Tl-rich regions are indicated by black and white, respectively.

Therefore, we conclude that the sharp drop of the contact line is not induced by the movement of the meniscus in the bulk but by the spreading of the wetting film.

This observation indicates that the wetting film of the Se-rich liquid phase intrudes between the Tl-rich phase and the quartz surface *when the temperature is decreased away from the critical temperature*. This result contrasts sharply with Cahn's critical point wetting theory [1], which predicts that the wetting film is formed *as the critical temperature is approached*. From now on, when the bulk Tl-rich phase is in direct contact with the quartz surface, we say that the system is in the 'non-wetting state', and when the Se-rich wetting film intrudes between them, we say that the system is in the 'wetting state'.

3.2. Wetting under the temperature gradient

Next, we studied the wetting behaviour under the temperature gradient, which was realized by heating the surface of the quartz cell. We have observed the liquid–quartz interface on changing T_{surf} at fixed T_{in}. Figures 5 and 6 show photographs taken at $T_{in} \simeq 400$ and 443 °C, respectively. Here, we defined the temperature difference ΔT as $T_{surf} - T_{in}$.

When T_{surf} is sufficiently higher than T_{in} (figures 5(a) and 6(a)), a flat contact line can be observed clearly, indicating that there is no wetting film on the liquid–quartz interface. The open circles in figure 4 show the height of the contact line observed when T_{surf} is much higher than T_{in} ($\Delta T \sim 20$ °C). It is noticed that they coincide closely with the position of the bulk meniscus h_{bulk}^{calc} (dashed line) calculated from the data in [15] under the assumption that the sample composition is precisely the critical composition (92.05 at.% Se). This result confirms that the wetting film is completely removed when ΔT is high enough.

When T_{surf} is decreased, we observed that the wetting film of Se-rich phase intrudes between the Tl-rich phase and the quartz wall. For example, when $T_{in} \simeq 400$ °C, the

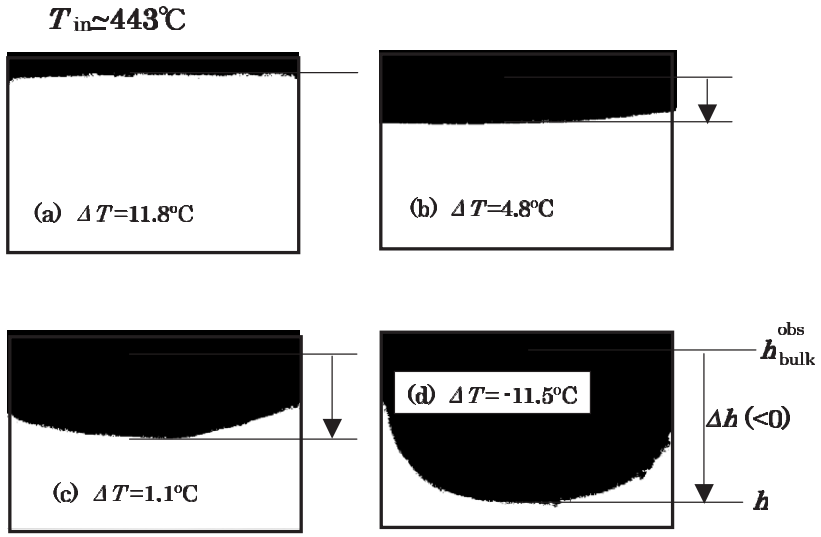

Figure 6. The binarized images of the liquid–quartz interface for various $\Delta T = T_{\rm surf} - T_{\rm in}$ at fixed $T_{\rm in}$ of 443 °C. The Se-rich and the Tl-rich regions are indicated by black and white, respectively. The definition of $\Delta h = h - h_{\rm bulk}^{\rm obs}$ is also indicated. Here, h is the observed height of the three phase contact line, and $h_{\rm bulk}^{\rm obs}$ is that measured at sufficiently high ΔT.

wetting film appears at $\Delta T = 7.4\,^{\circ}$C, forming complex wetting patterns (figure 5(b)). Below this temperature (figures 5(c) and (d)), the contact line disappears and the Tl-rich phase is completely covered with the Se-rich wetting film. It is noticed that the spreading of the wetting film takes place in a quite narrow ΔT region at $T_{\rm in} \simeq 400\,^{\circ}$C. On the other hand, when the $T_{\rm in}$ is close to the bulk critical point, the spreading of the wetting film becomes rather gradual. Figure 6 shows the liquid–quartz interface for various $T_{\rm surf}$ at fixed $T_{\rm in}$ of 443 °C. It is noticed that the area covered with the Se-rich wetting film spreads gradually downward with decreasing $T_{\rm surf}$.

From the binarized images we have calculated the fraction of the area, $P_{\rm cov}$, of the Tl-rich liquid phase covered with the Se-rich wetting film as a function of $T_{\rm in}$ and $T_{\rm surf}$. This calculation has been carried out by counting the number of black pixels, $N_{\rm black}$, in the binarized images. Then, $P_{\rm cov}$ is obtained by $P_{\rm cov} = (N_{\rm black} - N_{\rm black}^{\rm ref})/(N_{\rm tot} - N_{\rm black}^{\rm ref})$, where $N_{\rm tot}$ is the total number of the pixels, and $N_{\rm black}^{\rm ref}$ is the number of the black pixels when there is no wetting film. Figure 7 shows $P_{\rm cov}$ as a function of the temperature difference ΔT at various $T_{\rm in}$. In all cases, $P_{\rm cov}$ increases with decreasing ΔT. When $T_{\rm in}$ is lower than 430 °C, $P_{\rm cov}$ changes sharply from nearly zero to nearly unity at $\Delta T \sim 8\,^{\circ}$C, indicating that the transition from the non-wetting state to the wetting state is induced by the temperature difference ΔT. On the other hand, above $T_{\rm in} = 443\,^{\circ}$C, $P_{\rm cov}$ increases gradually with decreasing ΔT, and there is no discontinuous change in the covered area. It is also noticed that, in the homogeneous temperature conditions (i.e. $\Delta T = 0$), $P_{\rm cov}$ increases with decreasing $T_{\rm in}$, and becomes unity around 430 °C. This is consistent with the result described in section 3.1.

We define Δh $(=h - h_{\rm bulk}^{\rm obs})$ as the difference of the height of the three-phase contact line h from that of the bulk meniscus $h_{\rm bulk}^{\rm obs}$. The definition of Δh is illustrated in figure 6. As $h_{\rm bulk}^{\rm obs}$, we adopted the height of the contact line when ΔT is high enough and there is no wetting film, or the open circles in figure 4. Figure 8 shows the ΔT-dependence of Δh for various $T_{\rm in}$. It is noticed that the ΔT-dependence becomes gradual near the critical temperature, and this result

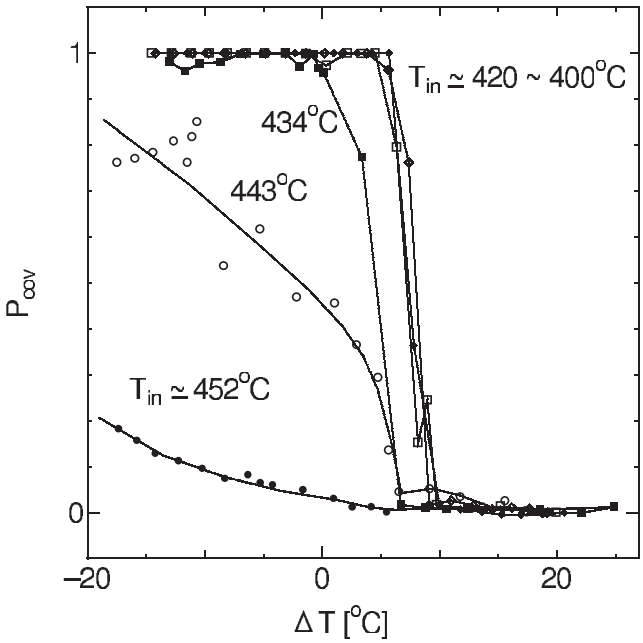

Figure 7. The fraction of the area of the Tl-rich liquid phase covered with the Se-rich wetting film, $P_{\rm cov}$, as a function of the temperature difference $\Delta T = T_{\rm surf} - T_{\rm in}$ at various $T_{\rm in}$. Solid circles, open circles, solid squares, open squares, solid diamonds and open diamonds represent $T_{\rm in} \simeq 452$, 443, 434, 420, 410 and 400 °C, respectively.

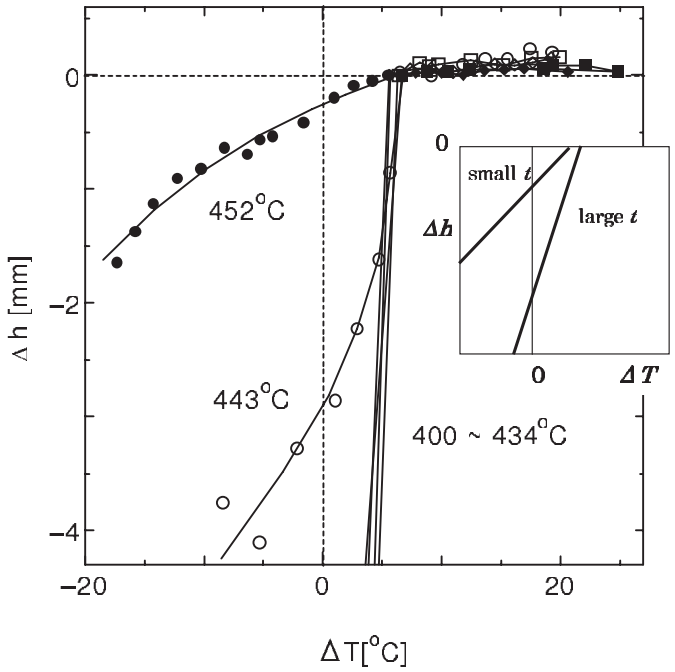

Figure 8. The ΔT-dependence of the height of the three phase contact line Δh relative to the bulk meniscus at various $T_{\rm in}$. The same symbols as figure 7 are used. The inset shows schematically the calculated boundary between the wetting and non-wetting states on the ΔT–$|\Delta h|$ plane (see (7)).

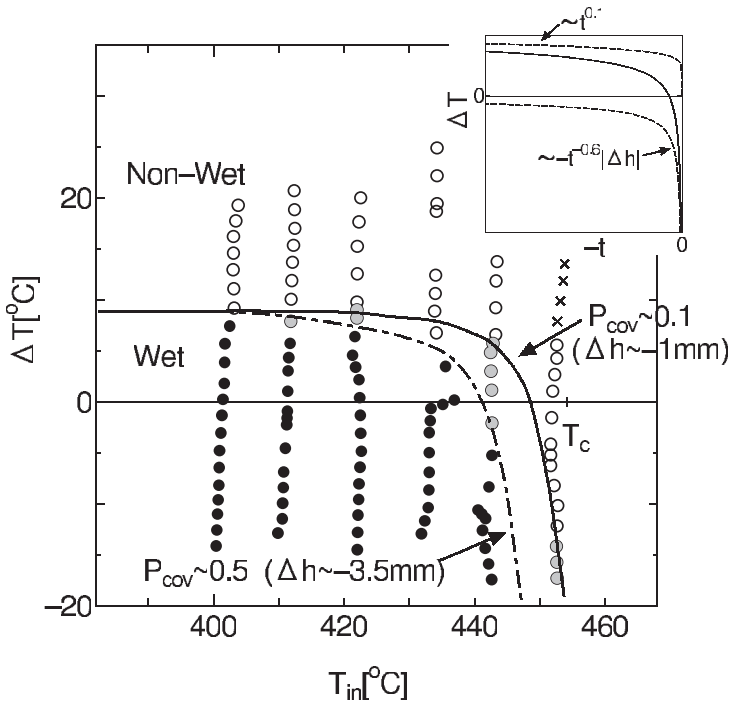

Figure 9. A summary of the experimental data points on the $T_{\rm in}$–ΔT plane. The open, grey and closed circles indicate the non-wetting ($P_{\rm cov} < 0.1$), partially wet ($0.1 < P_{\rm cov} < 0.5$) and the wetting ($P_{\rm cov} > 0.5$) state points, respectively. The crosses are the points where the liquid surface is in the one-phase region, and no contact line is observed. The solid curve separates the non-wet and partially wet regions, and the dash–dotted curve separates the partially wet and wet regions. $P_{\rm cov} = 0.1$ and 0.5 nearly correspond to $\Delta h = -1$ and -3.5 mm, respectively, for the data of $T_{\rm in} \simeq 443$ and 452 °C. The inset shows schematically the calculated boundary between the wetting and non-wetting states on the t–ΔT plane (see (6)).

suggests that downward spreading of the wetting film is blocked by the gravitational potential in this temperature region. The role of gravity in the critical point dewetting phenomena will be discussed later.

Figure 9 summarizes the experimental data points on the $T_{\rm in}$–ΔT plane. The points for the homogeneous temperature conditions (i.e. $\Delta T = 0$) are also plotted as special cases. As will be discussed in section 4.2, ΔT produces the difference of the chemical potential $\Delta\mu$ from the two-liquid coexistence value near the surface. From this point of view, we can say that figure 9 corresponds to the phase diagram on the $T_{\rm in}$–$\Delta\mu$ plane, which reflects the equilibrium properties of the system. The open and the closed circles indicate the non-wetting ($P_{\rm cov} < 0.1$) and the wetting ($P_{\rm cov} > 0.5$) state points, respectively. The grey circles are the state points where the wetting film partially covers the surface of the Tl-rich phase ($0.1 < P_{\rm cov} < 0.5$). $P_{\rm cov} = 0.1$ and 0.5 nearly correspond to $\Delta h = -1$ and -3.5 mm, respectively, for the data of $T_{\rm in} \simeq 443$ and 452 °C. The solid curve separates the non-wet and partially-wet regions, and the dash–dotted curve separates the partially wet and wet regions. The wetting state exists in the lower-$T_{\rm in}$ and lower-ΔT region. The solid and the dash–dotted curves intersect the line $\Delta T = 0$ at $T_{\rm in} \simeq 440$ and $\simeq$447 °C, respectively. Above this temperature, the Se-rich wetting film does not exist in the homogeneous temperature conditions ($\Delta T = 0$). Especially, the critical point ($T_{\rm in} = T_{\rm c} = 454$ °C and $\Delta T = 0$) is included in the non-wet region. This

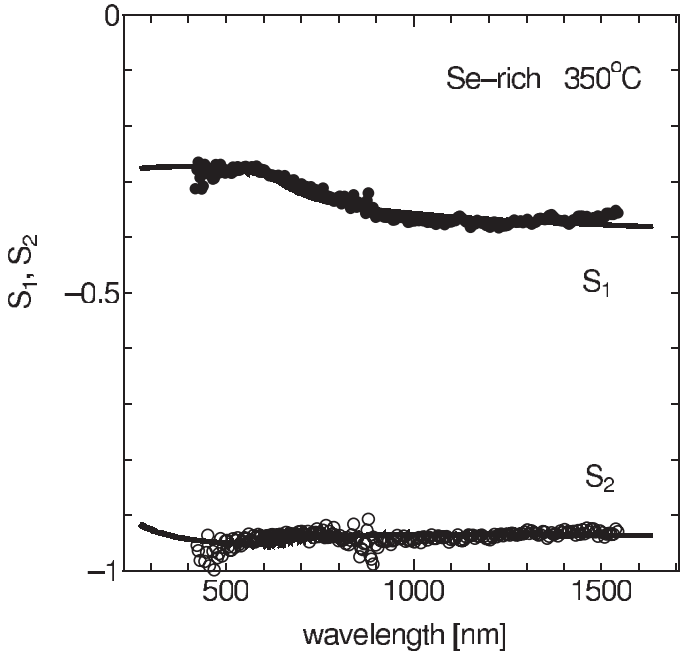

Figure 10. An example of the observed Stokes parameters $S_1(\lambda)$ (closed circles) and $S_2(\lambda)$ (open circles) for the Se-rich phase at 350 °C. The solid lines indicate the Stokes parameters calculated from the oscillator-fit method.

is consistent with the result of section 3.1 that there is no critical point wetting. It should be noted that the present systematic investigation in a wide range of ΔT indicates that the observed critical point dewetting is not induced by the temperature gradient but it is really an equilibrium phenomenon.

3.3. Ellipsometry

The ellipsometric measurements were made at various temperatures and at various heights of the light spot, z. In order to measure the optical constants for the Tl-rich phase at low temperature, the measurements were carried out near the bottom of the quartz cell, because the surface of the Tl-rich phase is nearly completely hidden under the Se-rich wetting film in the homogeneous temperature conditions, and only a small portion near the bottom of the cell is uncovered. In addition, the data at 300 °C were measured at T_{surf} slightly higher than T_{in} to remove the wetting film. Figure 10 shows an example of the observed Stokes parameters $S_1(\lambda)$ and $S_2(\lambda)$ for the Se-rich phase at 350 °C. The solid lines indicate the Stokes parameters calculated from the model dielectric function. The agreement between the observed and calculated Stokes parameters is fairly good in the wide wavelength region.

Figure 11 shows the complex dielectric functions at various temperatures for (a) Se-rich and (b) Tl-rich phases, obtained by the curve fitting analysis. When the temperature is decreased from 450 to 400 °C, the optical gap in the Se-rich phase (figure 11(a)) increases from 1.5 to 1.7 eV, accompanied by the decrease in the Tl concentration. Below 400 °C, the temperature change of the Tl content in the Se-rich phase becomes negligible, and the optical gap remains almost unchanged. Instead, the absolute value of both ϵ' and ϵ'' increases with

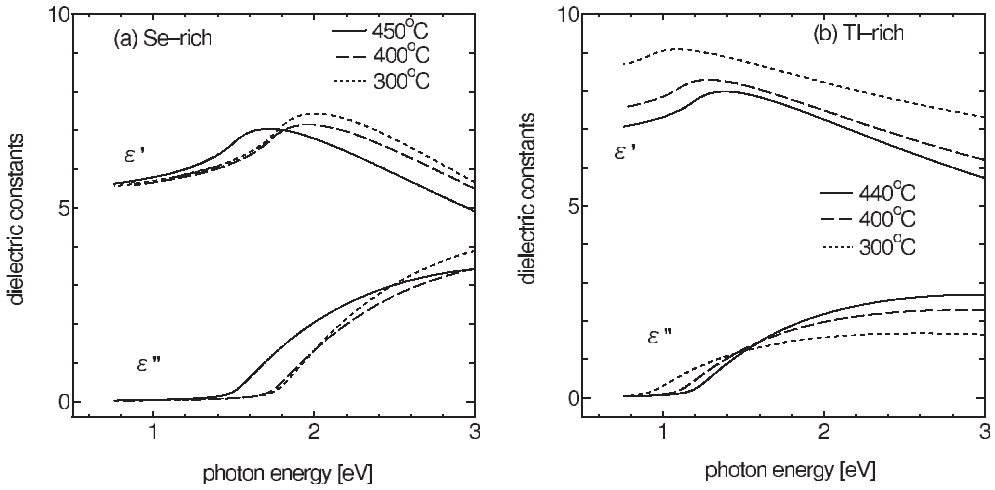

Figure 11. The complex dielectric functions at various temperatures for (a) Se-rich and (b) Tl-rich phases obtained by the curve fitting analysis to the ellipsometric data.

decreasing temperature. This trend below 400 °C is essentially the same as that observed for pure liquid Se [23].

On the other hand, the optical gap for the Tl-rich phase (figure 11(b)) decreases and the real part ϵ' of the dielectric constant increases monotonically when the temperature is decreased from 440 to 300 °C. This change in the $\epsilon(\omega)$ is accompanied by an increase in the Tl concentration in the Tl-rich phase with decreasing temperature.

We have also measured the optical constants of the Se-rich wetting film on changing the position of the light spot along the vertical coordinate z, and found that all the spectra are identical irrespective of the position, within the experimental error. In addition, we found no signs of the interference fringes in the spectra except for the position very close to the three-phase contact line (namely, the edge of the wetting film). These results indicate that the wetting film is uniform in composition, and is much thicker than the penetration depth of the light in the measured wavelength range.

4. Discussion

The observed critical point dewetting contrasts sharply with the Cahn's critical point wetting theory [1]. Cahn's argument is based on Young's equation and is quite simple. In the partial wetting state, the contact angle θ is expressed as

$$\cos\theta = \frac{\sigma_{1s} - \sigma_{2s}}{\sigma_{12}},$$

where σ_{ij} are surface tensions between i and j phases. The subscripts 1, 2 and s represent the Tl-rich phase, the Se-rich phase and the quartz substrate, respectively. As the critical temperature is approached, both numerator and denominator approach zero. The liquid–liquid surface tension vanishes as $\sigma_{12} \propto (T - T_c)^{2\nu}$ where ν is the critical exponent of the bulk correlation length [24] and it is equal to ~0.65 in a three-dimensional liquid. The difference in the liquid–substrate surface tensions between the two liquids, $\sigma_{1s} - \sigma_{2s}$, is considered to be due to the composition difference between the two liquids at the surface. Thus $\sigma_{1s} - \sigma_{2s} \propto (T - T_c)^{\beta_1}$, where β_1 is a surface critical exponent [25–27] which has the value

$\sim$0.8 [5]. Comparing these two temperature dependences, we see that $\cos\theta$ increases with temperature and reaches unity near the critical temperature, indicating the critical point wetting.

In order to interpret our experimental results, we construct a model grand potential, incorporating the long-range interaction, the temperature difference and gravity. The long-range interaction between the wetting film and the substrate is expected to be important in stabilizing the wetting film in the Se–Tl system. The long-range interaction is strong and highly temperature dependent, because the dielectric properties of the Se-rich and Tl-rich phases are substantially different and depend strongly on the temperature, as shown from the ellipsometric measurements. Furthermore, it is expected that gravity plays an important role in determining the boundary between the wetting and the non-wetting states, especially for a system with a large density difference between the two liquid phases. Indeed, the results of the T- and ΔT-dependence of the height of the three-phase contact line Δh (figure 8) suggest that the single use of the surface potential (long-range or short-range) is not sufficient to explain the observation, because the surface potential does not depend on the height, and it is necessary to take gravity into account.

4.1. The long-range force

In this subsection, we focus our attention on the long-range interaction. The free energy due to the long-range interaction, $W(l)$, per unit area of the wetting film depends on the film thickness l as $W(l) \sim -H/12\pi l^2$ for relatively large l when the retardation effect is neglected. (Note that the incorporation of the retardation effect (i.e. $W(l) \sim l^{-3}$) does not affect the following discussion.) Here, H is the Hamaker constant. For $l \to 0$, on the other hand, $W(l)$ approaches $\sigma_{1s} - \sigma_{2s} - \sigma_{12}$. From the general formula given by Dzyaloshinskii *et al* [28], the Hamaker constant is expressed as [29]

$$H = -\frac{3\hbar}{4\pi}\int_0^\infty \mathrm{d}\omega\, f(\mathrm{i}\omega), \tag{1}$$

where

$$f(\mathrm{i}\omega) = \frac{\epsilon_s(\mathrm{i}\omega) - \epsilon_2(\mathrm{i}\omega)}{\epsilon_s(\mathrm{i}\omega) + \epsilon_2(\mathrm{i}\omega)}\frac{\epsilon_2(\mathrm{i}\omega) - \epsilon_1(\mathrm{i}\omega)}{\epsilon_2(\mathrm{i}\omega) + \epsilon_1(\mathrm{i}\omega)}.$$

$\epsilon_1(\mathrm{i}\omega)$, $\epsilon_2(\mathrm{i}\omega)$, and $\epsilon_s(\mathrm{i}\omega)$ are dielectric functions for the Tl-rich bulk liquid phase, the Se-rich wetting film, and the quartz substrate, respectively, at imaginary frequencies $\mathrm{i}\omega$. $\epsilon(\mathrm{i}\omega)$ is calculated from the imaginary part of the dielectric function $\epsilon''(\omega)$ by using the relation

$$\epsilon(\mathrm{i}\omega) = 1 + \frac{2}{\pi}\int_0^\infty \mathrm{d}\omega' \frac{\omega'\epsilon''(\omega')}{\omega'^2 + \omega^2}.$$

Figure 12 shows $\epsilon(\mathrm{i}\omega)$ calculated from the ellipsometric data (figure 11) for Se-rich and Tl-rich phases at various temperatures. It is noted that the relation $\epsilon_s(\mathrm{i}\omega) < \epsilon_2(\mathrm{i}\omega) < \epsilon_1(\mathrm{i}\omega)$ is satisfied in a wide range of the frequency ω, and therefore H becomes negative. This result indicates that the long-range force prefers the Se-rich wetting film. When the temperature increases, $\epsilon_1(\mathrm{i}\omega)$ of the Tl-rich phase decreases sharply, indicating that the long-range force becomes weak near the critical point. However, this effect is not sufficient to explain the observed critical point dewetting, because the competing liquid–liquid surface tension σ_{12} also decreases when the critical point is approached.

4.2. The role of the temperature difference and the gravity

In the present work, we have introduced two external fields to control the surface states: the temperature difference $\Delta T = T_{\mathrm{surf}} - T_{\mathrm{in}}$ and gravity. In this subsection, we discuss the role of these two external fields.

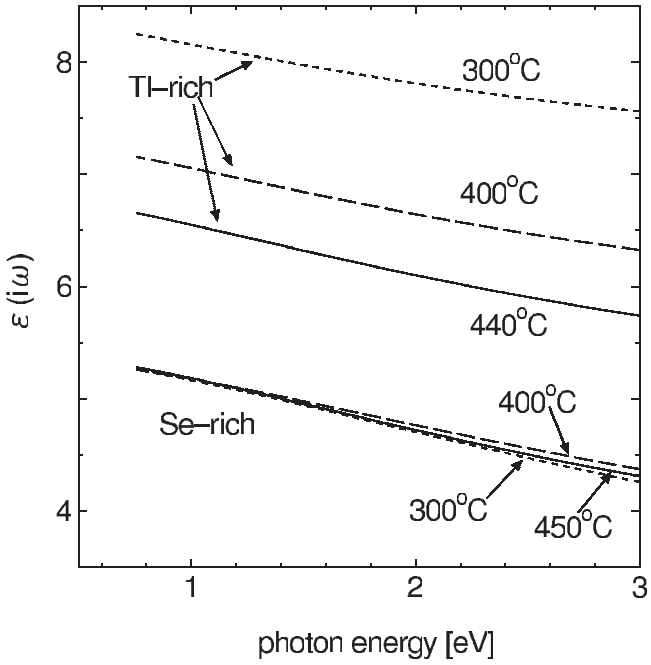

Figure 12. The dielectric functions $\epsilon(\mathrm{i}\omega)$ at the imaginary frequencies $\mathrm{i}\omega$ for Se-rich (lower part) and Tl-rich (upper part) phases at various temperatures. They are calculated from the ellipsometric data (figure 11). The solid, dashed and dotted lines indicate 450, 400 and 300 °C for Se-rich phase and 440, 400 and 300 °C for Tl-rich phase, respectively.

Let $c_{\mathrm{in}}^{\mathrm{Tl-rich}}$ and $c_{\mathrm{in}}^{\mathrm{Se-rich}}$ be the Se mole-fractions for the Tl-rich and the Se-rich phases deep inside the cell (i.e. bulk phases), respectively. In the present case, they are determined by the concentration on the coexistence curve, $c_{\mathrm{coex}}^{\mathrm{Tl-rich}}(T)$ and $c_{\mathrm{coex}}^{\mathrm{Se-rich}}(T)$, at $T = T_{\mathrm{in}}$, because the bulk phases deep inside the cell are in coexistence with each other. Along the coexistence curve, the *exchange* chemical potential [30] $\mu_{\mathrm{ex}}(c, T) = (\partial G_{\mathrm{m}}/\partial c)_{TP} = \mu_{\mathrm{Se}} - \mu_{\mathrm{Tl}}$ satisfies $\mu_{\mathrm{ex}}(c_{\mathrm{coex}}^{\mathrm{Se-rich}}(T), T) = \mu_{\mathrm{ex}}(c_{\mathrm{coex}}^{\mathrm{Tl-rich}}(T), T)$. Here, μ_{Se} and μ_{Tl} are the chemical potentials of the Se and Tl components, respectively, c is the Se mole-fraction, and G_{m} is the molar Gibbs free energy.

When the surface temperature is different from the bulk temperature, the coexistence condition is not satisfied locally near the surface. For example, when $T_{\mathrm{surf}} > T_{\mathrm{in}}$, the sample near the surface is in the one-phase region, indicating that the Tl-rich bulk phase is more stable compared to the Se-rich wetting film. The situation is depicted schematically in figure 13.

The Se mole-fraction of the Tl-rich liquid sample near the surface of the cell, $c_{\mathrm{surf}}^{\mathrm{Tl-rich}}$, is equal to $c_{\mathrm{in}}^{\mathrm{Tl-rich}} - (k_{\mathrm{T}}/T_{\mathrm{in}})\Delta T$, where k_{T} is the thermal diffusion ratio [31]. Unfortunately, we have no information on k_{T} for the Tl–Se system. However, it is known that k_{T} is small for many liquid systems[1]. If k_{T} can be neglected, $c_{\mathrm{surf}}^{\mathrm{Tl-rich}}$ becomes nearly equal to $c_{\mathrm{in}}^{\mathrm{Tl-rich}}$ $(=c_{\mathrm{coex}}^{\mathrm{Tl-rich}}(T_{\mathrm{in}}))$. This is smaller (larger) than $c_{\mathrm{coex}}^{\mathrm{Tl-rich}}(T_{\mathrm{surf}})$ for $\Delta T > 0$ $(\Delta T < 0)$.

When $c_{\mathrm{surf}}^{\mathrm{Tl-rich}} \neq c_{\mathrm{coex}}^{\mathrm{Tl-rich}}(T_{\mathrm{surf}})$, the difference in the exchange chemical potential from that at coexistence, $\Delta\mu_{\mathrm{ex}} = \mu_{\mathrm{ex}}(c_{\mathrm{surf}}^{\mathrm{Tl-rich}}, T_{\mathrm{surf}}) - \mu_{\mathrm{ex}}(c_{\mathrm{coex}}^{\mathrm{Tl-rich}}(T_{\mathrm{surf}}), T_{\mathrm{surf}})$, has a finite value. $\Delta\mu_{\mathrm{ex}}$

[1] In many aqueous solution systems, for example, $k_{\mathrm{T}}/(Tx)$ is of the order of 10^{-3} K^{-1}, where x is the concentration of the solute [32].

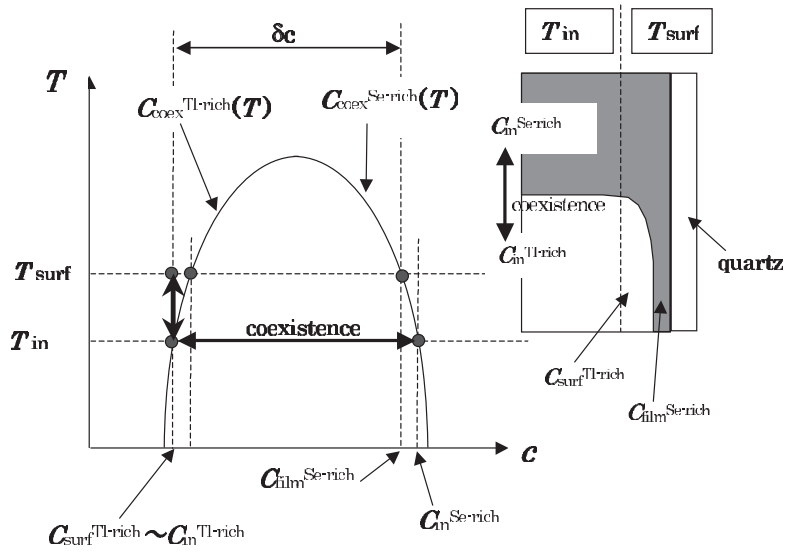

Figure 13. A schematic drawing showing the relation of the Se mole-fractions c at various positions in the cell when $T_{\rm surf} \neq T_{\rm in}$.

can be related to ΔT by using the following equation:

$$\begin{aligned}\Delta\mu_{\rm ex} &= \left(\frac{\partial\mu_{\rm ex}}{\partial c}\right)_{T=T_{\rm surf}} (c_{\rm surf}^{\rm Tl-rich} - c_{\rm coex}^{\rm Tl-rich}(T_{\rm surf})) \\ &\simeq \left(\frac{\partial\mu_{\rm ex}}{\partial c}\right)_{T=T_{\rm surf}} (c_{\rm coex}^{\rm Tl-rich}(T_{\rm in}) - c_{\rm coex}^{\rm Tl-rich}(T_{\rm surf})) \\ &\simeq -\left(\frac{\partial\mu_{\rm ex}}{\partial c}\right)_{T=T_{\rm surf}} \left(\frac{\partial c_{\rm coex}^{\rm Tl-rich}}{\partial T}\right)_{T=T_{\rm surf}} \Delta T. \end{aligned} \tag{2}$$

From the thermodynamic stability condition $(\partial^2 G_{\rm m}/\partial c^2)_{T,P} = (\partial\mu_{\rm ex}/\partial c)_{T,P} > 0$ and the slope of the coexistence curve $(\partial c_{\rm coex}^{\rm Tl-rich}/\partial T)_{T,P} > 0$, it is found that $\Delta\mu_{\rm ex}$ has a negative value for $\Delta T > 0$. Using this $\Delta\mu_{\rm ex}$, the additional free energy per unit area of the wetting film with thickness l because of the temperature difference is expressed as $-\Delta\mu_{\rm ex}\delta c\bar{n}l$, where δc is the difference in the Se mole-fraction between the two phases and $\bar{n}$ is the mean particle number density.

Next, we take gravity into account. When gravity is present, a wetting film with thickness l at the vertical coordinate z from the bulk meniscus has additional free energy $|\delta\rho g z|l$ per unit area. Here, $\delta\rho$ is the difference in the mass density between the two phases and g is the gravitational acceleration.

4.3. The phase boundary between the wetting and the non-wetting states

Summing up the terms discussed in the preceding subsections, we construct the grand potential $\Omega(l)$ per unit area when a Se-rich wetting film with thickness l is present between the Tl-rich bulk phase and the quartz substrate.

$$\Omega(l) - \Omega(0) = \sigma_{2\rm s} - \sigma_{1\rm s} + \sigma_{12} + W(l) + (|\delta\rho g z| - \Delta\mu_{\rm ex}\delta c\bar{n})l \tag{3}$$

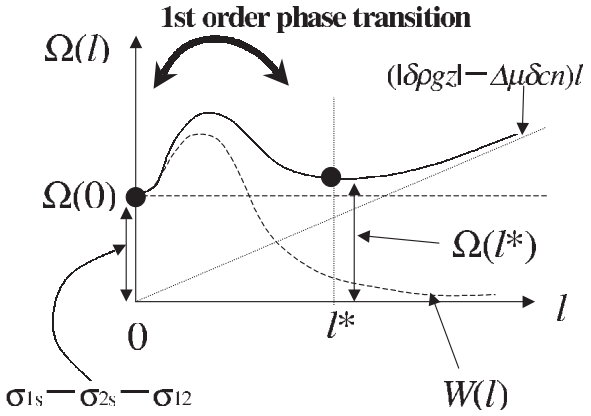

Figure 14. A schematic drawing of the grand potential $\Omega(l)$ as a function of the film thickness l. The two solid circles indicate the wetting ($l = l^*$) and the non-wetting ($l = 0$) states.

$$W(l) \simeq \begin{cases} -H/12\pi l^2 & \text{(for large } l\text{)} \\ \sigma_{1s} - \sigma_{2s} - \sigma_{12} & (l \to 0). \end{cases}$$

Figure 14 shows $\Omega(l)$ schematically. This grand potential has two minima: one is located at $l = 0$ [Note 2] and the other is at $l = l^* > 0$. The former corresponds to the non-wetting state, and the latter to the wetting state, where the film thickness l^* is limited by the $(|\delta\rho gz| - \Delta\mu_{ex}\delta c\bar{n})l$ term. l^* is obtained from the condition $(\partial\Omega/\partial l)|_{l=l^*} = 0$ as

$$l^* = \left(\frac{-H}{6\pi(|\delta\rho gz| - \Delta\mu_{ex}\delta c\bar{n})}\right)^{1/3}.$$

This expression is a natural extension of the equation $l^* = (-H/6\pi|\delta\rho gz|)^{1/3}$ given by de Gennes [33].

In many of the previous works on the thickness of a gravity-thinned wetting film, only the minimum of $\Omega(l)$ at $l = l^*$ has been taken into account. However, this is not sufficient to explain the observed dewetting. Indeed, in the homogeneous temperature condition (i.e. $\Delta T = 0$) and for a given height z, l^* does not depend on temperature [34, 11, 12, 35] because the critical exponent for the Hamaker constant is the same as that for the density difference $\delta\rho$ provided T is not very close to T_c. In addition, l^* varies continuously with z as $z^{-1/3}$ [34] and the well-defined three-phase contact line observed near T_c cannot be explained. In the present work, we have taken the other minimum at $l = 0$ into account in order to explain the transition between the wetting and the non-wetting states.

The difference in the grand potential between the wetting and the non-wetting states can be written as

$$\Omega(l^*) - \Omega(0) = \sigma_{2s} - \sigma_{1s} + \sigma_{12} + \frac{3}{2}\left(\frac{-H}{6\pi}\right)^{1/3}(|\delta\rho gz| - \Delta\mu_{ex}\delta c\bar{n})^{2/3}. \quad (4)$$

When $\Omega(l^*) - \Omega(0)$ is negative (positive), the wetting state is more stable (unstable) than the non-wetting state. Therefore, a first-order phase transition between these two states takes place when $\Omega(l^*) - \Omega(0)$ crosses zero. The phase boundary is given by such parameters (T_{in}, ΔT and $z = \Delta h$) that make $\Omega(l^*) - \Omega(0)$ zero.

[2] A very thin wetting layer possibly exists even in the non-wetting state. Such a situation can be easily taken into our theory without changing the final results by replacing the minimum at $l = 0$ by small but finite thickness $l = l^{**} \ll l^*$.

In the vicinity of the critical temperature T_c of the liquid–liquid phase separation, $\sigma_{1s} - \sigma_{2s}$ and σ_{12} depend on the reduced temperature $t = (T_c - T)/T_c$ as t^{β_1} and $t^{2\nu}$, respectively[3]. If there is no long-range interaction (i.e. $H = 0$), or both gravity and temperature difference are absent (i.e. $g|z| = 0$ and $\Delta T = 0$), the boundary between the wetting and the non-wetting states is determined by the two critical exponents β_1 and 2ν, and this coincides with Cahn's prediction. The situation changes, however, when the long-range interaction, gravity and the temperature difference are taken into account.

The two variables $|\delta\rho|$ and δc behave as $\sim t^{\beta}$, where $\beta \sim 0.33$ is the critical exponent for the three-dimensional order parameter. In addition, the Hamaker constant H is also expected to behave as $\sim t^{\beta}$, because, from (1), H is proportional to $\epsilon_2 - \epsilon_1$, which is expected to be proportional to δc near the critical point. From (2), $\Delta\mu_{ex}$ behaves as $\sim -t^{\gamma+\beta-1}\Delta T$, because $(\partial\mu_{ex}/\partial c)_T \sim t^{\gamma}$ and $(\partial c_{coex}^{Tl-rich}/\partial T)_{coex} \sim t^{\beta-1}$. Therefore, $-\Delta\mu_{ex}\delta c\bar{n} \sim t^{\gamma+2\beta-1}\Delta T \sim t^{1-\alpha}\Delta T$ ($\alpha \sim 0.10$). Using these relations, the grand potential can be written as

$$\Omega(l^*) - \Omega(0) \sim -At^{\beta_1} + Bt^{2\nu} + t^{\beta/3}(Ct^{\beta}|z| + Dt^{1-\alpha}\Delta T)^{2/3}, \tag{5}$$

where A, B, C, and D are positive proportional coefficients. The term $Bt^{2\nu}$ can be dropped for small t because the exponent $2\nu \sim 1.3$ is the largest among all the exponents in (5).

In the homogenous temperature condition (i.e. $\Delta T = 0$), $\Omega(l^*) - \Omega(0) \sim -At^{\beta_1} + t^{\beta}(C|z|)^{2/3}$ for $|z| \neq 0$. Because $\beta_1 \sim 0.8$ is larger than $\beta \sim 0.33$, it becomes positive for a sufficiently small t, indicating that *critical point dewetting* takes place for a system with finite $|z|$ and long-range force. This is a first-order phase transition accompanied by the discontinuous jump of the film thickness l from l^* to zero. It should be noted that the combination of gravity and the long-range force is necessary for critical point dewetting. Namely, the former prevents the film from thickening and the latter from thinning, and their combination pushes $\Omega(l^*)$ up compared to $\Omega(0)$. It is also interesting to note that the dewetting is closely related to the difference of the two critical exponents β_1 and β, and this strongly supports the idea that $\sigma_{1s} - \sigma_{2s}$ is controlled not by the critical exponent for the three-dimensional order parameter β but by the surface critical exponent β_1 [25–27, 5].

When a temperature difference ΔT is present, the phase boundary $\Omega(l^*) - \Omega(0) = 0$ is obtained from (5) as

$$\Delta T \sim \frac{A^{3/2}}{D}t^{\alpha+3\beta_1/2-\beta/2-1} - \frac{C}{D}t^{\alpha+\beta-1}|\Delta h| \sim \frac{A^{3/2}}{D}t^{0.1} - \frac{C}{D}t^{-0.6}|\Delta h|. \tag{6}$$

The phase boundary calculated from (6) is shown schematically in the inset of figure 9 on the t–ΔT plane. In the large-t (low-T) region, ΔT depends on t only weakly as $\sim t^{0.1}$ and does not depend on $|\Delta h|$. When t approaches zero, ΔT bends downward with the form $\sim -t^{-0.6}|\Delta h|$. In this region, ΔT depends strongly on $|\Delta h|$. This trend coincides well with that observed experimentally in figure 9. The typical parameters which nearly reproduce the observed boundaries are $A^{3/2}/D \sim 13$ K and $C/D \sim 2$ K cm^{-1}.

Similarly, the height of the three-phase contact line h is expressed as

$$\Delta h = -|\Delta h| = \frac{D}{C}t^{0.6}\Delta T - \frac{A^{3/2}}{C}t^{0.7}, \tag{7}$$

and is indicated schematically in the inset of figure 8, which shows that Δh changes linearly with ΔT. The slope of the line depends on t as $\sim t^{0.6}$, indicating that Δh changes sharply with

[3] In the ordinary fluid systems, β_1 cannot be used as the critical exponent of $\sigma_{1s} - \sigma_{2s}$ because the solid surface is covered by the wetting film near the critical point (Antonow's rule: $|\sigma_{1s} - \sigma_{2s}| = \sigma_{12} \sim t^{2\nu}$) [26, 27]. However, this rule cannot be applied to the Se–Tl system because the wetting film does not form up to the critical temperature. Sigl and Fenzl indicated that β_1 can be used as the critical exponent very close to T_c if the complete wetting is suppressed by adding KCl to the 2,6-lutidine–water system [5]. Following their results, we assumed in the present work that β_1 can be used as the critical exponent up to the critical temperature.

ΔT in the low-temperature (i.e. large-t) region, while it changes gradually when the critical point is approached. This trend is in agreement with the experimental result of figure 8.

We believe that the above mechanism is universal and can be applied to any system with a long-range force and gravity, when the concentration profile is sharp enough. The liquid Se–Tl system studied in the present work is especially suitable for observing the critical point dewetting, because it is a unique system with a combination of a large long-range force and a large mass density difference $\delta\rho$. In many binary fluid systems, on the other hand, no dewetting is observed up to very close to the critical temperature (for example, see [35]). In these systems, the dewetting may be covered up by the increase in the bulk correlation length, or critical adsorption.

5. Summary

We have studied the wetting phenomena of the liquid Se–Tl system on a quartz substrate by photography and ellipsometry. A thin layer of the Se-rich liquid phase intrudes between the Tl-rich liquid phase and the quartz substrate in the low-temperature region. However, the wetting film is not formed near the critical temperature, indicating the critical point dewetting. In addition, we have studied the wetting behaviour on changing T_{surf} independently of T_{in}, and found that the temperature difference ΔT induces the transition between the wetting and the non-wetting states. When the critical temperature is approached, the ΔT-dependence of the height $|\Delta h|$ of the three-phase contact line becomes rather gradual, and this result suggests that gravity is important in this system. From the ellipsometry, the optical constants of the Se-rich and the Tl-rich phases were measured, and the strong long-range force, which prefers the Se-rich wetting film, is predicted.

In order to interpret the observation, we constructed a model grand potential, incorporating the long-range interaction, the temperature difference and gravity. We found that this grand potential reproduces the observed behaviour qualitatively. From this analysis, it is suggested that the combination of the long-range force and gravity plays an important role in the observed critical point dewetting phenomena.

Acknowledgments

We would like to thank Mr K Tanaka for his collaborations on the experiment in the early stages. This work is partially supported by the Grant-in-Aid for the 21st Century COE 'Center for Diversity and Universality in Physics' from the Ministry of Education, Culture, Sports, Science and Technology (MEXT) of Japan, and by a grant-in-aid for Scientific Research (13740217, 14340106, 16540314) from the Ministry of Education, Culture, Sports, Science and Technology, Japan.

Appendix. Reflectivity of Se-rich wetting film

We have calculated the reflectivity R of the Se-rich wetting film between the quartz substrate and the Tl-rich bulk phase as a function of the film thickness l using the following equation:

$$R = \left| \frac{r_{\mathrm{s}2} + r_{21} \exp 2\mathrm{i}\Delta}{1 + r_{\mathrm{s}2} r_{21} \exp 2\mathrm{i}\Delta} \right|^2,$$

where

$$r_{\mathrm{ij}} = \frac{\tilde{n}_{\mathrm{i}} - \tilde{n}_{\mathrm{j}}}{\tilde{n}_{\mathrm{i}} + \tilde{n}_{\mathrm{j}}}$$

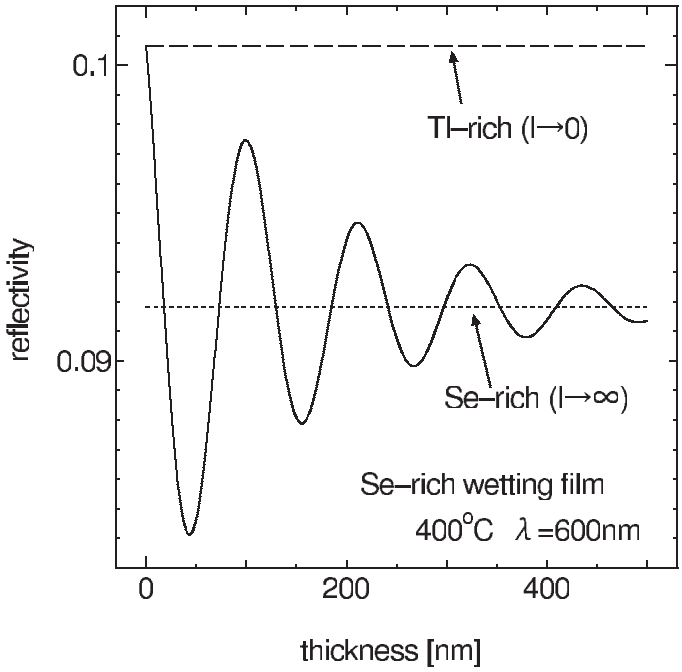

Figure A.1. The calculated reflectivity of the Se-rich wetting film between the quartz substrate and the Tl-rich bulk phase as a function of the film thickness. In this calculation, we used the optical constants obtained by the ellipsometry at 400 °C and the wavelength $\lambda = 600$ nm (figure 11). The dotted and dashed lines are the reflectivity of the bulk Se-rich and the Tl-rich liquid phases, respectively.

Figure A.2. A snapshot taken in the wetting process at $T_{\mathrm{in}} \simeq 300$ °C. At the rim of the Tl-rich phase, a dark coloured area due to the interference effect is observed.

and

$$\Delta = \frac{2\pi l}{\lambda}\tilde{n_2}.$$

The subscripts 1, 2 and s represent the Tl-rich phase, the Se-rich phase and the quartz substrate, respectively, $\tilde{n_i}$ $(i = 1, 2, s)$ is the complex refractive index of i phase, and λ is the wavelength of the light. Figure A.1 shows the result. In this calculation, we used the optical constants obtained by the ellipsometry at 400 °C and $\lambda = 600$ nm (figure 11). We found that a wetting film with a thickness of only a few tens of nanometres causes a large difference in the reflectivity

because of the large difference in the complex refractive index between the wetting film and the bulk phase. Indeed, the reflectivity decreases sharply with the thickness, and shows a minimum around 40–50 nm. This minimum is caused by the destructive interference of the light reflected from both sides of the film. At 400 °C, the reflectivity at the minimum is estimated to be ∼84% of that of the bulk Tl-rich surface. When the film thickness is increased further, the reflectivity oscillates and approaches the bulk reflectivity of the Se-rich phase, which is estimated to be ∼91% of that of the bulk Tl-rich surface. Therefore, the existence of the wetting film can be easily detected by direct observation.

Figure A.2 shows a snapshot taken in the wetting process at $T_{in} \sim 300\,^{\circ}C$. The Se-rich phase is intruding between the Tl-rich phase and the quartz from the outside. In this picture, a dark coloured area is observed at the rim of the Tl-rich phase. This dark area is caused by the interference effect, and the thickness of the wetting film in this area is estimated to be 40–50 nm.

References

[1] Cahn J W 1977 *J. Chem. Phys.* **66** 3667
[2] Nakanishi H and Fisher M E 1982 *Phys. Rev. Lett.* **49** 1565
[3] Bonn D and Ross D 2001 *Rep. Prog. Phys.* **64** 1085 and references therein
[4] Pohl D W and Goldburg W I 1982 *Phys. Rev. Lett.* **48** 1111
[5] Sigl L and Fenzl W 1986 *Phys. Rev. Lett.* **57** 2191
[6] Ebner C and Saam W F 1987 *Phys. Rev.* B **35** 1822
[7] Durian D J and Franck C 1987 *Phys. Rev. Lett.* **59** 555
Durian D J and Franck C 1987 *Phys. Rev.* B **36** 7307
[8] Abeysuriya K, Wu X and Franck C 1987 *Phys. Rev.* B **35** 6771
[9] Indekeu J O 1987 *Phys. Rev.* B **36** 7296
[10] Beaglehole D 1983 *J. Phys. Chem.* **87** 4749
[11] Wu X, Schlossman M and Franck C 1986 *Phys. Rev.* B **33** 402
[12] Bonn D, Kellay H and Wegdam G H 1992 *Phys. Rev. Lett.* **69** 1975
[13] Bonn D, Kellay H and Meunier J 1994 *Phys. Rev. Lett.* **73** 3560
[14] Pettit R B and Camp W J 1974 *Phys. Rev. Lett.* **32** 369
[15] Kanda F A, Faxon R C and Keller D V 1968 *Phys. Chem. Liquids* **1** 61
[16] Yao M and Hensel F 1996 *J. Phys.: Condens. Matter* **8** 9547
[17] Yao M and Ohmasa Y 2001 *J. Phys.: Condens. Matter* **13** R297
[18] Ohmasa Y, Kajihara Y and Yao M 2000 *Phys. Rev.* E **63** 051601
[19] Ohmasa Y, Takahashi S, Fujii K, Nishikawa Y and Yao M 2006 *J. Phys. Soc. Jpn* **75** 084605
[20] Aspens D E and Studna A A 1975 *Appl. Opt.* **14** 220
[21] Huard S 1997 *Polarization of Light* (Chichester: Wiley and Masson)
[22] Ohmasa Y, Fujii K, Takahashi S and Yao M 2006 to be published
[23] Silva L A and Cutler M 1990 *Phys. Rev.* B **42** 7103
[24] Widom B 1965 *J. Chem. Phys.* **43** 3892
[25] Binder K 1983 *Phase Transitions and Critical Phenomena* vol 8, ed C Domb and J Lebowitz (London: Academic) p 1
[26] Pandit R, Schick M and Wortis M 1982 *Phys. Rev.* B **26** 5112
[27] Sullivan D F and Telo da Gamma M M 1986 *Fluid Interfacial Phenomena* ed C A Croxton (New York: Wiley)
[28] Dzyaloshinskii I E, Lifshitz E M and Pitaevskii L P 1961 *Adv. Phys.* **10** 165
[29] Israelachvili J N 1991 *Intermolecular and Surface Forces* 2nd edn (London: Academic) chapter 11
[30] de Gennes P G 1979 *Scaling Concepts in Polymer Physics* (Ithaca, NY: Cornell University Press) chapter IV.2.1
[31] Landau L D and Lifshitz E M 1959 *Fluid Mechanics* (London: Pergamon) chapter VI
[32] Fitts D D 1962 *Nonequilibrium Thermodynamics* (New York: McGraw-Hill) chapter 9
[33] de Gennes P G 1981 *J. Physique Lett.* **42** L377
[34] Kwon O'D, Beaglehole D, Webb W W, Widom B, Schmidt J W, Cahn J W, Moldover M R and Stephenson B 1982 *Phys. Rev. Lett.* **48** 185
[35] Fenistein D, Bonn D, Rafai S, Wegdam G H, Meunier J, Parry A O and Telo da Gamma M M 2002 *Phys. Rev. Lett.* **89** 096101